

Article

Efficiency and Reliability Assessment-Based Selection of the Optimal Common Bus in Hub-Stations

Hira Tahir ^{1,*}, Hasan Erteza Gelani ¹, Muhammad Saleem ^{2,3} and Asif Hussain ⁴

¹ Department of Energy Engineering, University of Engineering and Technology, New Campus, Kala Shah Kaku 39020, Pakistan; erteza.gelani@uet.edu.pk

² Department of Electronics Engineering Technology, The Benazir Bhutto Shaheed University of Technology and Skill Development, Khairpur Mirs 66020, Pakistan; msmemon13@hanyang.ac.kr

³ Department of Electrical Engineering, Hanyang University, Seoul 04763, Republic of Korea

⁴ Department of Electrical Engineering, University of Management and Sciences, Lahore 54000, Pakistan; asif.hussain@umt.edu.pk

* Correspondence: hira.tahir@uet.edu.pk

Abstract: This paper is an attempt to present a simple yet innovative planning method for determining the type of common bus in a hub station (HS), devised on efficiency and reliability grounds. The efficiency is evaluated by modeling the efficiency curves of the converters under part-load and full-load conditions, hence enabling a realistic estimate of the efficiency. Reliability evaluation is executed by modeling the failure and repair rate distributions of the HS components. The optimal common bus type selection is based on both the efficiency and reliability metrics of the HS. The deterministic factor in the type of common bus selection is proved to be the number of components in the HS. The results indicate that DC and AC systems have comparable efficiencies with a meagre difference of 1.26%. The failure rate of AC common bus architecture is 22% greater than DC common bus architecture resulting in a 1.788 times reliability advantage of the DC system. Moreover, the greater number of components in the case of a AC common bus adds to the economic advantage of DC with a lower number of components leading DC to be an optimal design.

Keywords: AC versus DC; common bus; efficiency; hub station; Monte Carlo simulation; reliability



Citation: Tahir, H.; Gelani, H.E.; Saleem, M.; Hussain, A. Efficiency and Reliability Assessment-Based Selection of the Optimal Common Bus in Hub-Stations. *Electronics* **2023**, *12*, 3411. <https://doi.org/10.3390/electronics12163411>

Academic Editors: Shriram Srinivasarangan Rangarajan and E. Randolph Collins

Received: 9 July 2023

Revised: 8 August 2023

Accepted: 9 August 2023

Published: 11 August 2023



Copyright: © 2023 by the authors. Licensee MDPI, Basel, Switzerland. This article is an open access article distributed under the terms and conditions of the Creative Commons Attribution (CC BY) license (<https://creativecommons.org/licenses/by/4.0/>).

1. Introduction

As conventional generating centers are located far from load centers, transmission lines with a high capacity are required to supply a substantial amount of load. In lieu of creating new transmission lines, the installation of hub stations (HSs) near load centers is a cost-effective means of bridging the ever-widening supply-demand gap. In addition, the global community is reducing CO₂ emissions to combat climate change spurred on by global warming and rising average temperatures. Therefore, the Green New Deal is being advocated, which aims to replace the industrial structure based on fossil fuels with eco-friendly energy by gradually lowering CO₂ emissions by 2050. Accordingly, governments intend to meet a substantial portion of overall power demand with renewable energy resources (RERs) such as photovoltaic (PV), wind, and fuel cells (FC). In addition to RERs, the shifting trend towards electric vehicles (EV) has significantly reduced carbon emissions. Charging EVs with renewable energy reduces emissions even further [1]. On the basis of these considerations, the literature has recommended PV and FC-based HS to fulfill electric vehicle charging station (EVCS) load demand [2].

The system as a whole can be described as shown in Figure 1. The HSs integrate RERs, energy storage system (ESS), and load, creating a hub-like node that facilitates local generation and utilization. The benefits are two-fold. First, RERs are used instead of conventional generators to reduce CO₂ emissions and combat climate change caused by global warming. Second, the cost of constructing transmission lines to supply distant loads

is reduced. The RERs supply the HS with power via a medium voltage direct current (MVDC) line. These HSs are interconnected. Through the MVDC line, the surplus/deficit output power of each HS may be supplied/absorbed to/from neighboring HS. In addition, each HS is connected to the primary utility grid (UG) by means of AC transmission lines. When power from RERs and other HSs is inadequate to fulfil the load demand, the UG delivers power to the EVCS load.

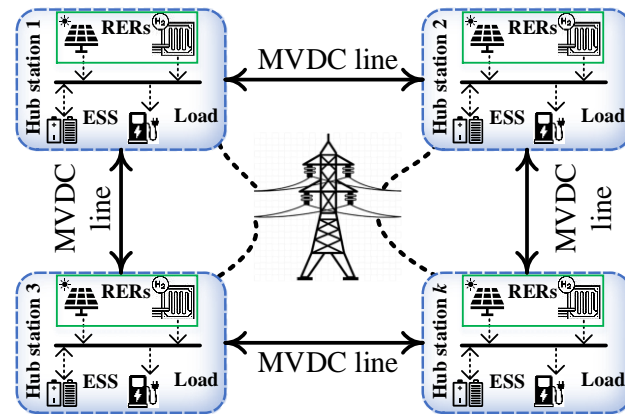


Figure 1. Overall framework of the system.

The RERs, ESS, EVCS load, and UG are coupled by power electronic (PE) interfaces to a common bus. The common bus is the backbone of HS and is responsible for power distribution among HS components. Choosing the appropriate type of common bus substantially increases the design performance. Important design considerations include efficiency, reliability, cost, and power quality, among others. This paper considers efficiency and reliability as deciding factors for the common bus type, as they frequently conflict with one another during design optimization. Despite the fact that these two are related, they are not the same. Efficiency is the degree to which input is effectively used, whereas reliability is the length of time a system operates without failing. Efficiency refers to the increase in output, whereas reliability stresses the likelihood of failure. It is possible to obtain high efficiency under unreliable conditions and vice versa. A system that experiences numerous failures of extremely short duration, for example, can have low reliability without sacrificing efficiency greatly. Analogously, a system can have much lower output, but it seldom fails. When optimizing a design, efficiency and reliability are often at odds, and a compromise can be made to find the optimal solution. Based on the above arguments, it is imperative to analyze the prospective HS at the early design stage with regards to efficiency and reliability to determine the common bus type.

This research effort addresses the loopholes in previous research efforts by determining the optimal common bus type for the HS based on both evaluations of efficiency and reliability. The efficiency of the HS is obtained by evaluating the efficiency of the converters under part-load and full-load conditions, whereas the reliability is determined by modeling and simulating the failure and repair rate distributions of the converters using Monte Carlo simulations. Based on the results of both analyses, the optimal type of common bus for the HS is selected. The authors believe that the entire process will serve as a guide for design engineers to determine the optimal common bus type for HSs/microgrids prior to moving into real-world implementation. Below is a comparison between the proposed method and previous research efforts.

1.1. Comparison with Previous Research

Efficiency evaluation of a system has been a subject of many researchers. As the cornerstone of distribution systems, the efficiency of a system is largely dependent on the efficiency of PE converters. The author presented a study based on a fixed efficiency drop of 2.5% for each conversion stage. However, the effect of load variation on the efficiency of the

converters has not been touched [3]. Starke et al. [4] performed loss comparison for the two paradigms: AC versus DC. The findings revealed that when loads are divided equally, i.e., 50% AC and 50% DC loads, both systems have the same benefits. Nonetheless, the authors asserted fixed efficiency of the converter, despite the load variation. Sannino et al. [5] determined that a DC voltage of 326 V is optimal for the existing AC system. However, only line losses were taken into account, with converter efficiencies neglected. Anand and Fernandes [6] compared the performance of DC systems with that of conventional AC systems. The appropriate voltage levels for residential and commercial systems were found in account of the fixed conversion efficiencies. Fregosi et al. [7] examined AC and DC microgrids using sophisticated validated simulation models. However, the study's scope was confined and did not take into account converter efficiencies under varying loading. Backhaus et al. [8] utilized average conversion efficiencies and recommended an extensive simulation-based analysis taking part-load conditions into account. The authors of [9] analyzed the efficiency of RER-based AC and DC microgrids (MGs) and developed an analysis-based selection principle based on static converter efficiencies. In addition to the previously mentioned literature, Dastgeer and Gelani [10] presented a comparative analysis of AC and DC residential systems including static converter efficiency. The present body of knowledge contains analyses that either take into account average or statics converter efficiencies. This necessitates a model that incorporates the impact of percentage loading into the efficiency curve of the converter to assess the system's efficiency accurately and realistically.

A meagre number of publications deterministically modeled the efficiency curve of converters for system efficiency evaluation. For instance, Gerber et al. [11] conducted comprehensive parametric simulations for efficiency analyses. Gelani et al. authored a number of publications addressing the efficiency analysis considering residential localities [12–21]. In Indonesia's shift to renewable energy, Saputra et al. [22] conducted an efficiency study of DC and AC MGs. The results demonstrated a substantial dependence on the efficiency of the converters. A few authors conducted an efficiency analysis of the system employing a statistical approach [23,24]. Likewise, the authors in [25] employed copula function-based efficiency curves of the converters to determine the most favorable common bus under various scenarios. Although the authors considered the impact of load variation to fairly imitate the variable and nonlinear relation between converter loading and efficiency; efficiency alone cannot be regarded as pivotal in determining the optimal common bus type, as previously illustrated. The system must be evaluated for both efficiency and reliability to reach a final verdict.

Alongside efficiency evaluation, reliability analysis has also been a focus of attention of several researchers. For instance, the authors of [26] evaluated the reliability of the system and found that as the number of components decreases, reliability increases. Reliability of a real microgrid comprising PV and FC is measured in [27]. The approaches used are reliability block diagrams (RBD), fault tree analysis (FTA), and Markov reliability modeling (MRM). The impact of component reliability on large scale PV system's performance was analyzed in [28] using FTA. A reliability, availability, and maintainability analysis for grid-connected PV systems was studied using RBD in [29]. A combined efficiency and reliability analyses of AC and DC distribution in data centers is presented in [30]. The authors derived the component's loss models for efficiency calculations. Failure and repair rate distributions were sampled for reliability analysis. In evaluating the reliability of systems, analytical and numerical approaches predominated. However, these techniques are impracticable for complicated systems with a significant number of series and parallel connections due to the extensive calculations required. Monte Carlo simulations have been extensively used in the literature. Due to the simplicity and relative ease of implementation, it is still being applied to predict the system's reliability and behavior [31]. In addition to the above-cited literature, the system's reliability has recently been examined in [32–36]. However, the optimal type of common bus for the HSs cannot be determined based solely on the reliability evaluation.

The optimal selection of the common bus is a vital early design decision that must consider both efficiency and reliability.

1.2. Organization of This Paper

The remainder of this paper is outlined as follows: Section 2 discusses the system under discussion, whereas Section 3 presents the efficiency evaluation method. Section 4 describes the modeling process for converter efficiency curves. A method for reliability analysis is described in Section 5. Section 6 describes the case study, followed by results and analysis in Section 7. Section 8 concludes the paper, while Section 9 addresses the limitations of this work and provides recommendations for the future.

2. System Description

The current article takes a PV and FC-powered HS into consideration. The HS is configured in a radial topology since it allows for simple source/load integration and scaling possibilities without requiring extensive modification. The RERs provide power to the HS through an MVDC line, with appropriate utilization of conversion stages. By way of a bidirectional converter, the ESS is linked to the common bus. The ESS serves as a load when power by RERs exceeds load demand and otherwise as a source.

The prevalence of RER-based MGs and efficient electronic converters has led to the tendency to shift to DC loads, replacing the AC counterparts as LED TVs, lights, and even household motor-based appliances, etc. Therefore, it is not unreasonable to conclude that the current system is heading toward DC [37]. Consequently, it is fair to undertake the relative efficiency analysis exclusively for DC loads. In our analysis, we therefore considered DC load as illustrated in Figure 2. Transportation is responsible for 14% of worldwide GHG emissions, according to statistics. As a result, EV proliferation has been advocated in order to reduce carbon emissions that lead to global warming [38,39]. In this article, EVCS load is therefore regarded as a DC load.

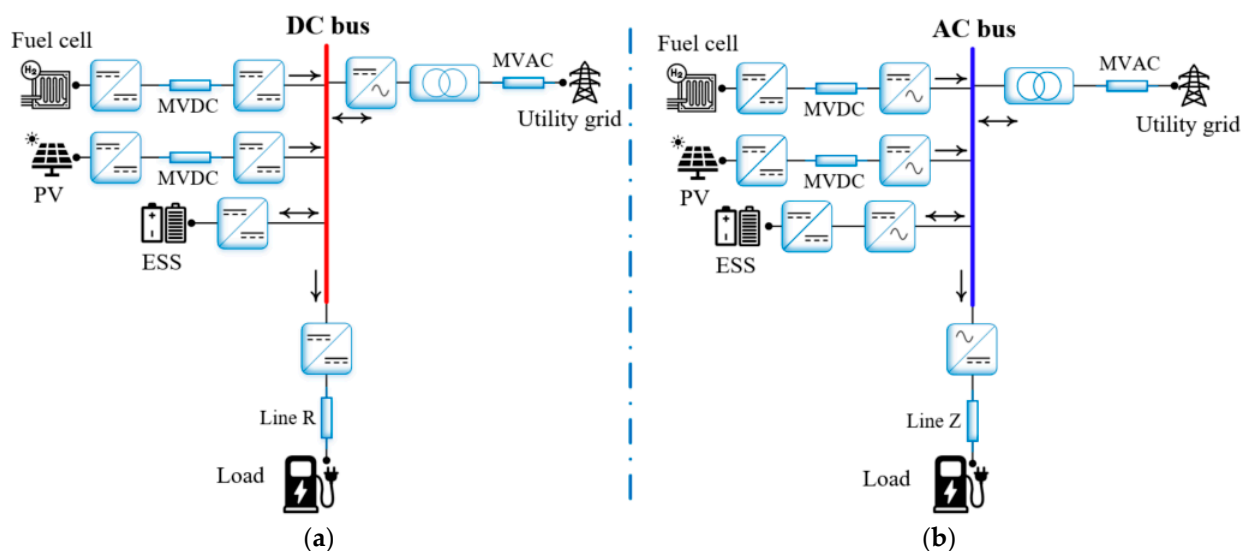


Figure 2. Single HS diagram for: (a) DC common bus; (b) AC common bus.

Figure 2 presents the overall system. Figure 2a presents an HS with a DC common bus. At the FC and PV generators, DC–DC converters are utilized for generation to DC common bus conversion. The connection of medium voltage alternating current (MVAC) UG to the common bus is built through a conversion stage of DC–AC converter and conventional transformer. Figure 2b is the AC counterpart of Figure 2a. Along with the DC–DC converters, the generating side also includes DC–AC converters for conversion. A DC load is provided at the load side through an AC–DC conversion stage. The DC–AC

converter on the grid side is eliminated, and an additional DCAC conversion stage is employed on the ESS end.

Sustaining a balance between generation and consumption is one of the requirements for reliable operation of HS, which is disturbed by the intermittent nature of RERs. In the literature, a variety of solutions are presented to address this issue, such as load shifting, shedding, management, and utilization of ESS, etc. [40–43]. The current paper proposes a technique that employs ESS to enhance the reliability of HS and optimize consumption of RERs along with optimal energy extraction from the UG. Nonetheless, the performance of the ESS is highly dependent on high or low state of charge (SoC) [44], leading to lower overall performance of the HS. The ESS capacity is designed with an adequate margin to perform optimally while working within normal SoC limitations of 20–80%. When the SoC is beyond the safe working limits, extra or insufficient power is delivered to or absorbed by the UG respectively, hence preserving its operational integrity. HS converters operate substantially below their rated capacity leading to lower conversion efficiency, which adversely affects the HS's overall efficiency. Therefore, the current analysis establishes a comparative evaluation of AC and DC HS, based on the efficiency of converters.

3. Efficiency Evaluation Method for the HS

The overall efficiency of the HS is contingent on the efficiency of each component. Instantaneous power is required to be determined in order to furnish the percentage loading of the converter, for each instant. The procedure is executed in line with the scheme, as depicted in Figure 3. The HS can operate in three modes according to the generated power and load demand. The ESS is considered to be completely charged at the beginning of the day.

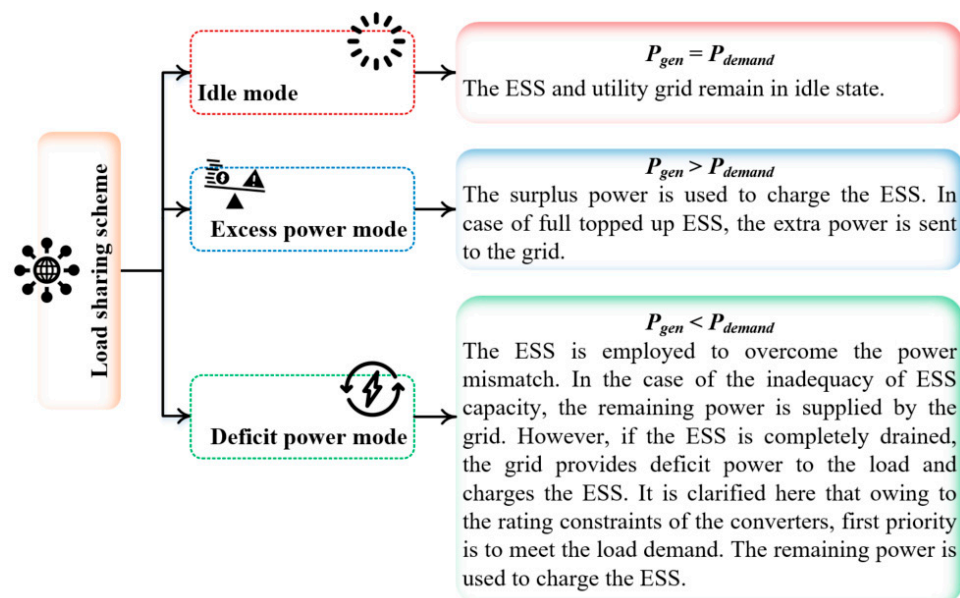


Figure 3. Load sharing scheme for the HS.

Idle mode is enabled when generated power, P_{gen} , i.e., sum of the power from FC and PV, equals load demand, P_{demand} , at any given time instant. In this instance, neither the ESS nor the grid contribute to supplying the load demand. Consequently, the instantaneous power of the associated converters is zero. The instantaneous power of the rest of the converters is determined by the power generation from the corresponding source. When P_{gen} exceeds P_{demand} , the HS works in excess power mode. On the contrary, when P_{gen} is less than the P_{demand} , deficit power mode is enabled.

After determining the instantaneous power in line with the scheme of Figure 3, HS efficiency may be estimated using the steps explained below.

The percentage loading can be defined mathematically as:

$$l_{\%}^i = \frac{P_{conv}^i}{P_{rated,conv}} \quad (1)$$

where $P_{rated,conv}$, P_{conv}^i , and $l_{\%}^i$ represent the nominal power of the converter, instantaneous power, and percentage loading of the converter at i th time instant, respectively. Here, i defines hour of the day.

After determining the percentage loading of each converter, the hourly efficiency of the converter against this percentage loading is computed using the efficiency curve model described in the next section. The dissipated power of each converter may then be evaluated using Equation (2).

$$Loss_{conv}^i = P_{conv}^i \times (1 - \eta_{conv}^i) \quad (2)$$

where $Loss_{conv}^i$ and η_{conv}^i represent the instantaneous loss and efficiency of the converter at i th time instant, respectively. Calculation of the power dissipated in R/Z and MVDC line is as follows:

$$Loss_{line}^i = 2 \times \left(I_{line}^i \right)^2 \times R \quad (3)$$

$Loss_{line}^i$ is the instantaneous lost power in the distribution line, and I_{line}^i represents the current passing through the line. The loss of each component is then integrated to determine the total power loss of the HS, on an hourly basis. The total dissipated power in the converters and lines can be computed by:

$$Loss_{total}^i = \sum_{conv} Loss_{conv}^i + Loss_{line}^i \quad (4)$$

where, $Loss_{total}^i$ is the total power dissipated in the HS at i th time instant. The EVCS power consumption represents the output of HS per hour. Ultimately, the overall efficiency, η_{HS}^i , is acquired using:

$$\eta_{HS}^i = \frac{P_{demand}^i}{Loss_{total}^i + P_{demand}^i} \quad (5)$$

Integrating the factors of operational efficiency, instantaneous power, and distribution loss yields the overall loss of HS. Ultimately, efficiency is obtained by Equation (5). An accurate evaluation of the HS's efficiency necessitates the actual behavior of the converter's efficiency curve.

4. Converters' Efficiency Curve Modeling

The precision and accuracy of the efficiency model of each component are interrelated. The actual efficiency of any component of an HS varies as load varies. The converters' efficiency is an important determinant in HS's overall power loss. Therefore, the efficiency curves of converters must be precisely modeled. The typical efficiency curves of converters demonstrate the efficiency decrement at extremely light loads, swift rise at medium loads, and almost fixed at full loads. Therefore, correct efficiency models must be derived in order to provide precise estimates of efficiency. The efficiency of power converters may be represented as in Equation (6).

$$\eta_{conv} = f(l_{\%}) \quad (6)$$

The polynomial function yields a good fit for empirical data, depicted as:

$$f(l_{\%}) = \sum_{j=0}^m \alpha_j (l_{\%})^j \quad (7)$$

where $m = 6$ for all type of converters and α_j are the efficiency coefficients that are deduced through curve fitting of the data provided by the manufacturers at various load levels. Based on the type of converter and its prospective application, the reference efficiency curves are obtained from the past research for all types of converters in the HS. For analysis, the efficiency curves of HS converters such as source side DC–DC converters, source side DC–AC converters, ESS bidirectional DC–DC converters, ESS bidirectional DC–AC converters, load side DC–DC converters, load side AC–DC converters, and grid side DC–AC converters were taken from [13,45–49], respectively. Figure 4 provides the efficiency vs. percentage loading curves for these converters.

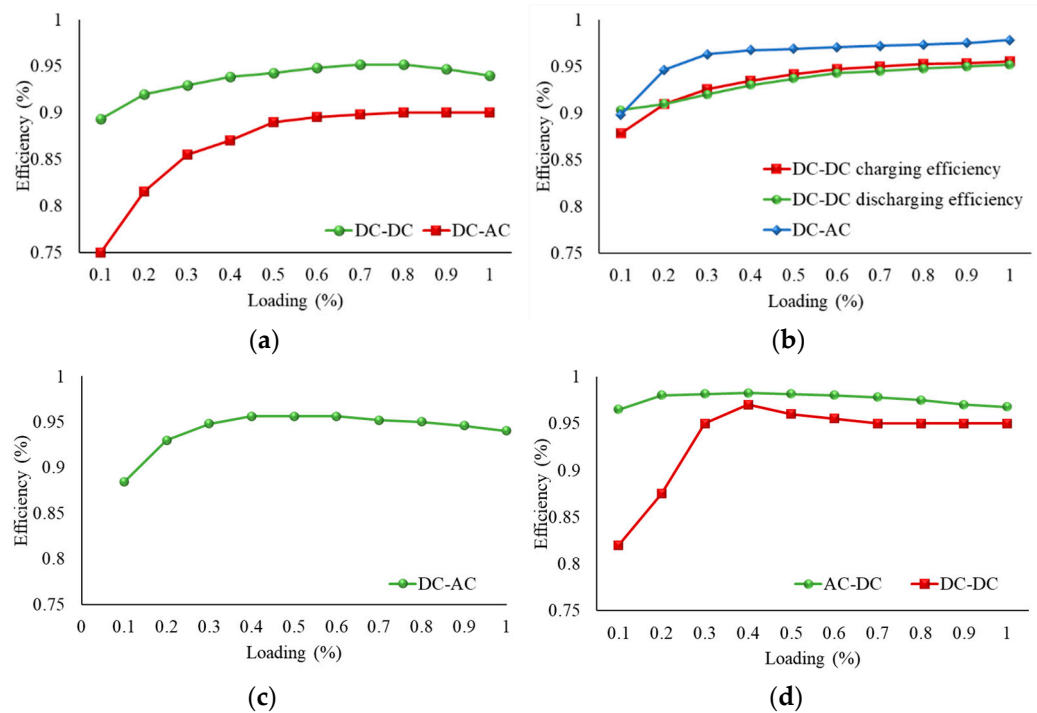


Figure 4. Efficiency curves of converters in HS: (a) Source side converters; (b) ESS converters; (c) Grid side converters; and (d) Load side converters.

It is evident from the curves that efficiency varies with percentage loading in quite a nonlinear fashion. However, the efficiency of AC transformers conventionally ranges from 95% to 98% [13], which leads to a minor loss. In this analysis, the AC transformer loss is thus disregarded. The efficiency coefficients derived from curve fitting of these curves are listed in Table 1. Using these efficiency coefficients, efficiency of the converter, η_{conv} , against percentage loading, $l_{\%}$, can be easily obtained using Equation (7). Once the efficiency at i th time instant is available, efficiency of the HS can be computed by following the procedure described in the previous section. Figure 5 summarizes the whole process of efficiency calculation of the HS. By following these steps, efficiency of the HS for the AC and DC common bus is computed. The results for efficiency analysis are discussed in Section 7.

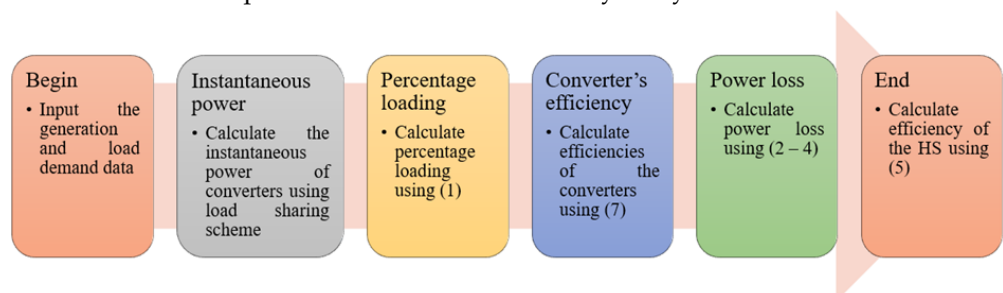


Figure 5. Efficiency calculation process.

Table 1. Efficiency coefficients of converters.

Component		Efficiency Coefficients						
		α_0	α_1	α_2	α_3	α_4	α_5	α_6
Source side	DC–DC conv.	0.829	0.0942	−0.0373	0.0081	−0.0009	6×10^{-5}	-1×10^{-6}
	DC–AC conv.	0.6215	1.7581	−0.0581	0.012	−0.0015	1×10^{-4}	-2.57×10^{-6}
Grid side DC–AC conv.		0.7821	1.4469	−5.2219	10.621	−12.697	8.2308	−2.222
Load side	AC–DC conv.	0.92	0.0699	−0.031	0.007	−0.0008	5×10^{-5}	-1×10^{-6}
	DC–DC conv.	0.9722	−0.3771	0.3076	−0.0965	0.0146	−0.0011	3×10^{-5}
ESS bidirectional DC–AC conv.		0.7856	0.1619	−0.059	0.0112	−0.0012	6×10^{-5}	-1.3×10^{-6}
ESS bidirectional DC–DC conv.	Charging	0.8129	0.0923	−0.0325	0.0067	−0.0008	5.00×10^{-5}	-1.00×10^{-6}
	Discharging	0.9055	−0.0087	0.0078	−0.0013	5.00×10^{-5}	4.00×10^{-6}	-3.00×10^{-7}

5. Survival Function Modeling and Reliability Analysis

Reliability has always been a prime concern in the design of electrical systems. It is defined as the likelihood that a component will continue to function under certain conditions over a specified amount of time. Component type, quality, stress level, and number have a significant impact on the total system reliability. The greater the number of components in a system, the more prone it is to fail. Moreover, the accuracy of reliability estimation depends on the robustness of the failure distribution model of each component. For reliability calculations, power system components typically follow an exponential distribution [50]. Throughout their operational lifespan, it is assumed in this study that the failure rate and repair rate of all components are constant, and that their distribution functions are exponential. The failure and repair rates are denoted by λ (failures/year) and μ (repairs/year), respectively. The cumulative failure rate of HS, λ_{cum} , is computed by using the parts count reliability prediction method [51].

$$\lambda_{cum} = \sum_x N_x (\lambda_g \times \pi_q)_x \quad (8)$$

where x represents the type of HS component, N is the number of components, λ_g is the generic failure rate, and π_q is the quality factor of the corresponding component. Reliability, also known as survival function, can be modeled as:

$$S(t) = e^{-\lambda_{cum}t} \quad (9)$$

or it is equal to the product of reliability of individual HS components.

$$S(t) = \prod_x e^{-\lambda_x t} \quad (10)$$

The failure rates of the HS components considered for survival function modeling in this work are presented in Table 2. To simplify, π_q is assumed as one for each component. For reliability calculations, thousands of random scenarios were generated using Monte Carlo simulations. Finally, the HS reliability for the DC and AC common bus is computed using Equation (10) over a period of twenty-five years of operation. The findings of the reliability analysis of the HS for both the AC and DC common bus are presented in Section 7.

Table 2. The component generic failure rate.

Failure Rate (yr) ^{−1}	DC–DC	DC–AC	AC–DC	Transformer	ESS	UG
	0.0066	0.1643	0.0164	0.0004	0.0137	0.0411

6. Case Study

For comparing the common bus configurations based on efficiency and reliability analysis, we considered an HS with a AC and DC common bus shown in Figure 2. As mentioned earlier, the trend is shifting towards DC appliances/loads. Therefore, in our comparative analysis, the DC loads are considered only. The following subsections describe the daily load demand pattern, generated power, and HS specifications.

6.1. Load Demand

The EVCS load data is designed considering South Korean public charging stations. Over 95% of charging stations in South Korea utilize Tesla superchargers, i.e., level 3 charging. Table 3 presents the EVCS load statistics used in this work [52]. Monte Carlo simulations have been employed to predict the load demand for public charging stations using these data. Monte Carlo simulation uses random variables to estimate the likelihood of uncertain parameters by conducting several simulations. Each uncertain parameter is sampled by a random number whose distribution matches that of the uncertain parameter. The system is subsequently simulated several times. Each simulation yields a system realization that describes the future of the system.

Table 3. Data for EVCS load demand calculation.

Charger Type	Nominal Voltage (V_{dc})	Current (A)	No. of Slots/Charging Station	Max. Power Rating/Slot (kW)
Tesla Supercharger	480	300	4–6	120

The EVCS load modeling presented in this article is supported by [53], which anticipates the demand for charging stations in various regions using ride-hailing trip data. The current article analyzes load patterns for public charging stations during holidays and weekends to account for maximum load demand. It is assumed that the number of slots in a charging station and the number of EVs connected at once are uncertain parameters. Moreover, they adhere to the distribution pattern described in [53]. Using Monte Carlo simulation, eight charging stations have been simulated in total. For simulation modeling, a plethora of software packages, each with distinct features, are available. For instance, MATLAB, PSS/E, @RISK, and DiGSILENT, etc. The @RISK simulation program (provided by Palisade Decision Tools Suite) has a proven potential to simulate thousands of random scenarios, hence enabling important insights into the model. In this work, @Risk simulation software is employed for EVCS load modeling. While we used this software for the current study, other options may also be used depending on the research objectives, available resources, and familiarity with the software. The EVCS load demand during a 24-h period is depicted in Figure 6. In computations, the 95th percentile load demand is considered.

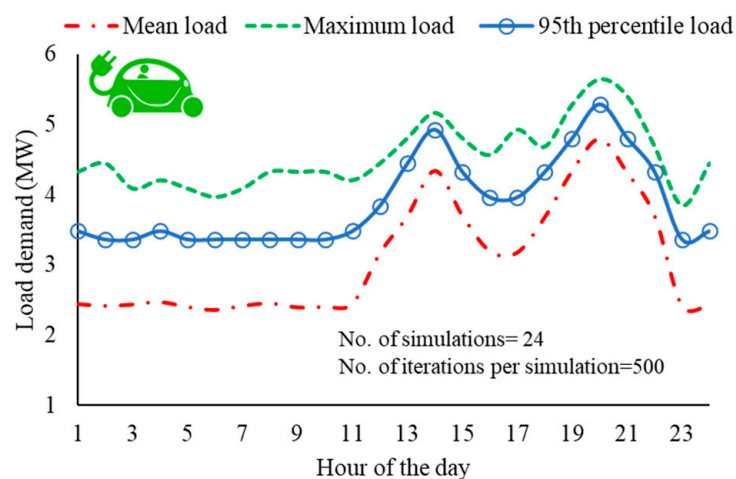


Figure 6. EVCS daily load demand curve.

6.2. FC and PV Generation

Fuel cell technology is now in the spotlight because of its exceptional reliability, efficiency, environmental friendliness, and noiselessness. Yet, this technology is not ideal due to its high cost, sensitivity to impurities, and deterioration over time. Despite these drawbacks, the combination of environmental concerns, technological advancements, and supportive policies has put fuel cell technology in the spotlight, driving increased interest and investment in its development and implementation. As research and innovation continue, the drawbacks of fuel cell technology are likely to be addressed further, paving the way for broader adoption and integration into various sectors. In recent years, global research interests have been primarily focused on proton exchange membrane (PEM) and solid oxide fuel cell (SOFC) stacks. This article, therefore, considers PEM fuel cells with a total capacity of 5 MW and an overall efficiency of 85% [54]. Typically, the voltage variation in a stack of fuel cells is within 20% [55]. Monte Carlo simulations have been used to create the fuel cell generated power. Here, it is considered that the fuel cell works constantly, and its output is distributed uniformly.

The PV generated power used in this paper is based on a 50 MW solar power plant [30] that was scaled down to 5 MW for this study. Figure 7 depicts the FC generated power for a day and hourly solar power plot for January 4 (worst-case scenario).

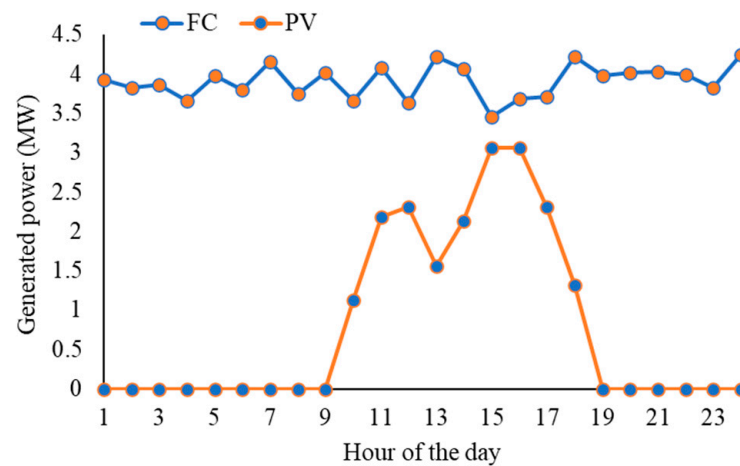


Figure 7. Generated power in the HS.

6.3. HS Specifications

The HS studied in this work is depicted in Figure 2. Table 4 provides a list of RERs rated capacity, proximity from HS, common bus voltages, and MVAC and MVDC line rated voltages. Studies employed 380 V DC in their analysis due to the accessibility of components with appropriate ratings, safety requirements, the amount of battery cells, and the insulation level of cables [30,56,57]. Similarly, when comparing the DC common bus voltage to the AC common bus, we used 380 V.

Table 4. HS specifications.

Component	Value
DC bus voltage (V)	380
AC bus voltage (V)	220
Voltage of MVDC line (kV)	2
Voltage of MVAC line (kV)	22.9
Distance of PV from HS (km)	4.4
Distance of FC from HS (km)	1.4
Distance of load from HS (km)	10
PV rating/Nominal voltage (MW/kV)	5/6
FC rating/Nominal voltage (MW/kV)	5/6

Table 5 outlines the characteristics of the overhead transmission lines used for determining the power loss in the MVAC and MVDC lines [58,59]. In this study, conventionally used ACSR/AW conductors for overhead transmission lines are employed. Owing to local generation and local consumption, the distribution network is quite compact. Therefore, resistance of the common bus may be disregarded. The findings of the efficiency and reliability evaluation of the HS are subsequently presented.

Table 5. Line parameters.

Line	Impedance
R/Z (Ohm/km)	R = 0.4842; X = 0.4388
MVAC (Ohm/km)	R = 0.4842; X = 0.4388
MVDC (Ohm/km)	R = 0.1110

7. Results and Discussion

7.1. Efficiency Analysis

The efficiency analysis of HS is segregated in two parts: efficiency analysis with the DC common bus and efficiency analysis with the AC common bus. Figure 8 depicts the power loss in each component of HS for both cases in descending order. In the case of the DC common bus and the AC common bus, the load side and source side converters experience the most power loss, respectively. Figure 9 shows the HS efficiency comparison for both scenarios. Despite the fact that additional DC–AC converters are utilized at the source and ESS side, the efficiency of HS with the AC common bus is systematically greater than that with the DC common bus. In the case of the AC common bus, the greatest and lowest efficiency values were 79.25% and 66.25%, respectively, whereas for the DC common bus, the values were 76.63% and 67.73%, respectively.

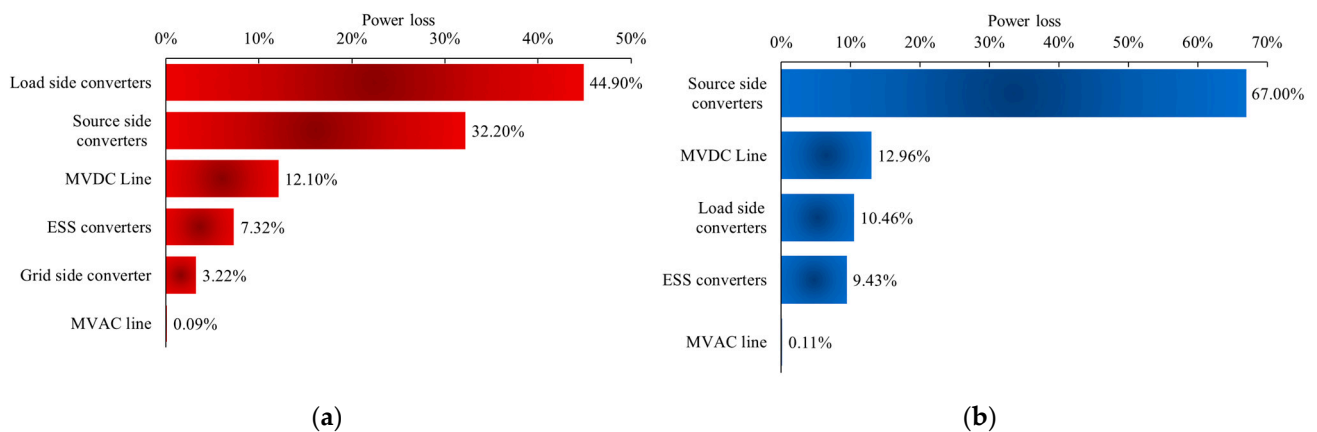


Figure 8. The loss breakdown in the HS: (a) DC common bus; (b) AC common bus.

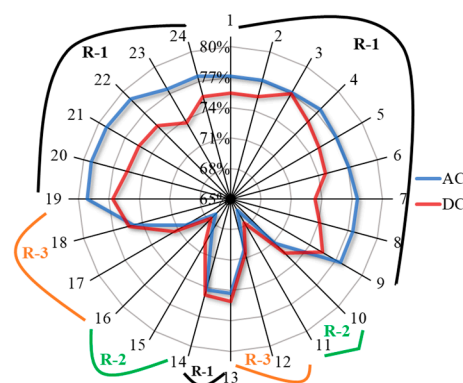


Figure 9. HS hourly efficiency graph.

The efficiency plots for both cases have a comparable general trend. These are segmented into three regions.

7.1.1. Region 1 (R-1)

The efficiency curve from 1st till 9th hour of the day is nearly constant in the case of the AC common bus; however, it slightly varies for the DC common bus. Likewise, from hour 13th till 14th and 19th till 24th, the efficiency follows a similar trend for both cases. The reason for the consistent value is the non-availability of PV generation during this period of time. Because there are fewer converters involved, the overall power loss is less. The FC, ESS, and UG cater to the whole EVCS load in accordance with the load sharing scheme described in Section 3.

7.1.2. Region 2 (R-2)

The efficiency starts to drop between the 10th–11th and 15th–16th hour of the day. Despite the increase of PV, the efficiency has decreased in the former time span owing to greater power dissipation in the PV converters as compared to generation contribution. During the subsequent time period, the excess power is available at the common bus. Consequently, it is used to recharge the ESS. However, the lower percentage loading of the ESS converters results in more power loss and a decline in overall efficiency.

7.1.3. Region 3 (R-3)

The efficiency rises during the 12th and 17–18th hours. At the 12th hour, the significant boost in PV generation leads to the improved efficiency of the system. The increase in efficiency is noticed due to the gradual diminishing of PV power, causing less power loss in the PV converters during the 17–18th hours of the day.

The efficiencies averaged over the day for both cases differ by around 1.26%, with the AC outperforming the DC over the majority of the day.

7.2. Reliability Analysis

The reliability of the HS for both the AC and DC common bus was modeled with the @Risk simulation tool with the failure rates listed in Table 2. A total of 25 simulations were made with 50,000 iterations per simulation. The failure rate of HS with the DC common bus was found to be 17.33×10^{-3} failures/year, whereas for the AC common bus, it was 22.26×10^{-3} failures/year. The failure rate with the DC common bus is 22% less than that with the AC common bus.

Figure 10 shows the reliability of HS components for both of the cases over 25 years of operations. A swift decline in reliability is seen for the DC–AC converter in both situations. This converter has the maximum likelihood of failure, turning out to be the least reliable component of the HS. Along with the higher failure frequency, the larger number of this converter in the case of the AC common bus worsens the reliability metrics. The transformer is the least vulnerable to failure, proving to be the most reliable component throughout the operational years.

We performed the sensitivity analysis to analyze the impact of the component's failure rate on the HS's reliability. The results are presented in Figure 11. The longest bar corresponds to the component with the highest impact on average reliability of HS. DC–AC converters contribute the most in HS reliability degradation. The second biggest contribution to the HS failures is the UG followed by the AC–DC and DC–DC converter in the case of DC and AC common bus, respectively.

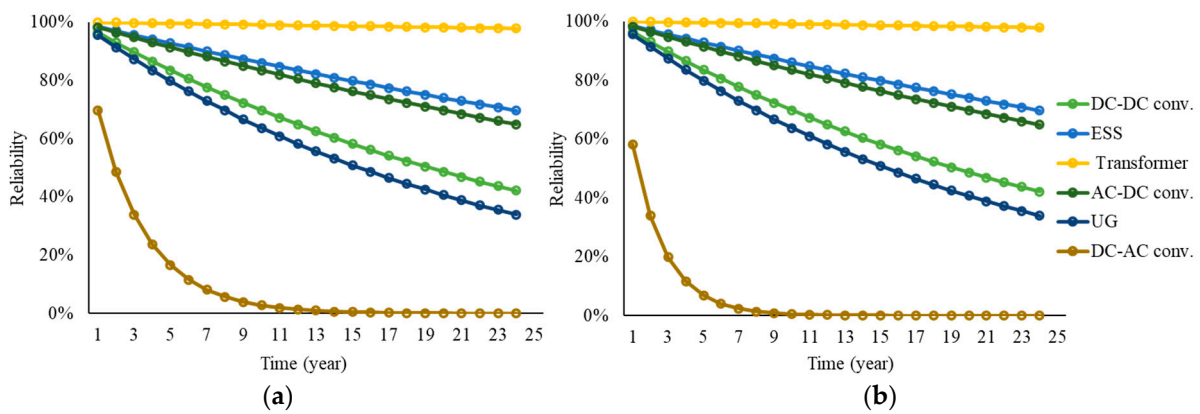


Figure 10. Reliability metrics of HS components for: (a) DC common bus; (b) AC common bus.

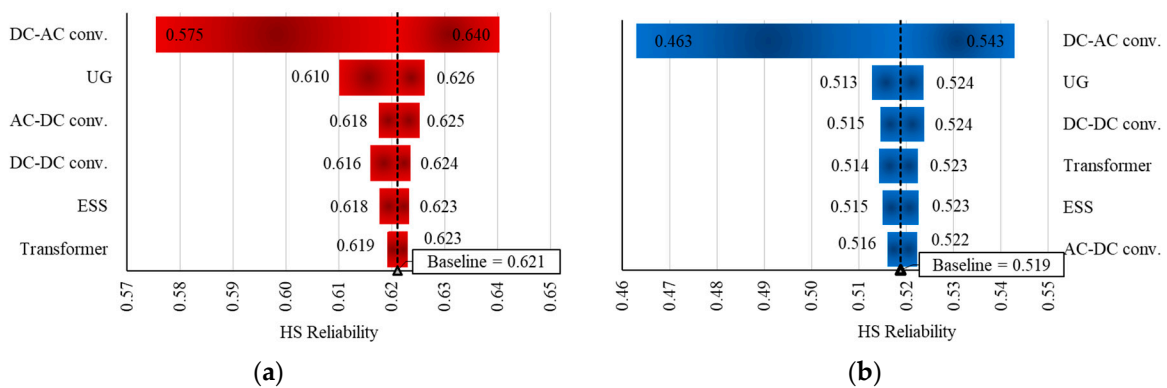


Figure 11. Share of component's failures in average reliability of HS for: (a) DC common bus; (b) AC common bus.

The overall reliability of HS for the DC and AC common bus is compared in Figure 12. The DC common bus is far more reliable than its AC counterpart. The average reliability of the two systems differs by 7.88%, with the DC common bus exhibiting 62.16% and the AC common bus showing 54.28% reliability, respectively.

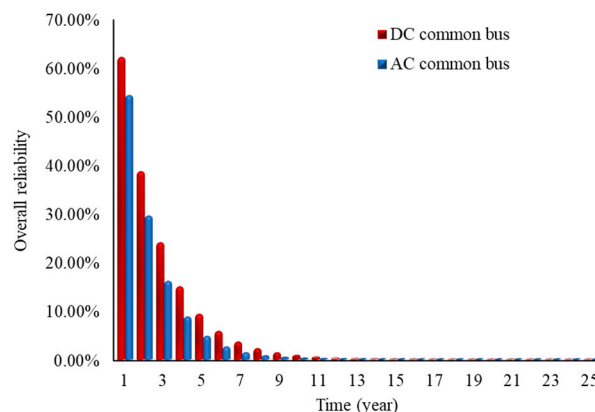


Figure 12. HS reliability comparison for 25 years of operations.

8. Conclusions

This paper developed the efficiency and reliability analysis of a HS for the selection of common bus. The component's loss and survival function models have been devised for efficiency and reliability analysis, respectively. The average efficiency of HS for both of the systems is commensurable with a tiny difference of 1.26%. There are instances when

efficiency is constant, decreasing, and increasing. The first region corresponds to the time span of the day when there is no solar power available and all the load is supplied by FC, ESS, and UG. The drop in efficiency is observed during the time interval when the PV contribution to the total generation is less as compared to the escalated losses due to the large number of converters engaged. The efficiency bar improves in the period of a noteworthy rise in PV generation. However, the critical component in defining the efficiency of HS is the load side DC–AC converter. The absence of this converter is the potential reason for the higher efficiency despite the increased number of converters employed in the case of the AC common bus.

On the contrary, the reliability metrics for the DC common bus are much better than its AC peer. The larger the number of components, the more susceptible is the system to collapse early. The HS with the DC common bus is 1.788 times more reliable.

Figure 13 presents the comparison between reliability and efficiency of HS for both scenarios. The positive number demonstrates DC's superiority over AC. The reliability metrics are a cut above the efficiency numbers in defining the type of common bus. Although both of the systems are equally efficient to some extent, the DC common bus presents a way more reliable HS than the AC common bus.

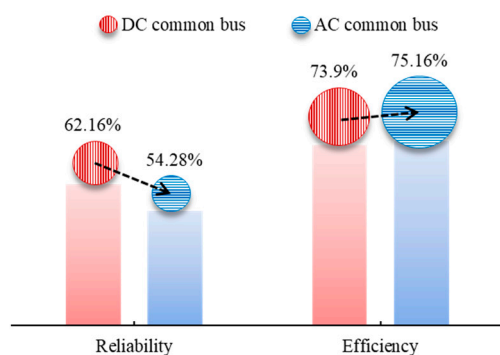


Figure 13. Quantitative comparison between reliability and efficiency numbers (proportional to the size of circle).

To summarize, HS with the DC common bus offers fair efficiency and higher reliability. Moreover, the higher proportion of converters required for the AC common bus will add to the total cost of the HS. Hence, HS with the DC common bus is concluded as the optimal design.

9. Limitations and Future Recommendations

This study assessed efficiency and reliability to select the most suitable common bus for the HS. While this study provides valuable insights, it is important to acknowledge its limitations. The authors have only evaluated two of the design factors discussed in Section 1 for determining the optimal common bus type. Other factors alongside these two can be analyzed to reach a conclusion. For example, power quality, a prime concern while integrating the RERs into the power system, as discussed in [60]. The authors were not able to include the best-case scenario for the generation and load profile, which limits the comprehensive evaluation of the system's reliability. In future studies, the authors intend to include the best-case scenario to provide a more comprehensive evaluation of reliability. PE converters with a modular architecture may help achieve a balanced solution based on efficiency and reliability, as both will increase simultaneously in this case. A risk–benefit analysis can help identify the potential causes of the system's low average reliability and efficiency. In addition, econometric analysis can be used to determine the cost benefits of the potential common bus type. Ideally, a techno-economic analysis would include the trade-off between performance and savings; that is one of our potential research directions.

Author Contributions: Conceptualization, H.T.; methodology, H.T.; software, H.T.; validation, H.T., H.E.G., M.S. and A.H.; formal analysis, H.T.; investigation, H.T.; resources, H.E.G. and M.S.; data curation, H.T. and A.H.; writing—original draft preparation, H.T.; writing—review and editing, H.E.G., M.S. and A.H.; visualization, H.T., H.E.G. and M.S. All authors have read and agreed to the published version of the manuscript.

Funding: This research received no external funding.

Data Availability Statement: Not applicable.

Conflicts of Interest: The authors declare no conflict of interest.

References

1. Longo, M.; Foadelli, F.; Yaïci, W. *Electric Vehicles Integrated with Renewable Energy Sources for Sustainable Mobility*; IntechOpen: London, UK, 2012.
2. Park, S.S.; Lee, J.S.; Park, D.H.; Kim, R.Y. Hierarchical Structure-based Ramp rate Control of Renewable Energy Sources for Hub-Station. In Proceedings of the ICEMS 2021—2021 24th International Conference on Electrical Machines and Systems, Gyeongju, Republic of Korea, 31 October–3 November 2021; Institute of Electrical and Electronics Engineers Inc.: New York, NY, USA, 2021; pp. 808–811.
3. Hammerstrom, D.J. AC versus DC distribution systems—did we get it right? In Proceedings of the 2007 IEEE Power Engineering Society General Meeting, Tampa, FL, USA, 24–28 June 2007; pp. 1–5.
4. Starke, M.; Tolbert, L.M.; Ozpineci, B. AC vs. DC distribution: A loss comparison. In Proceedings of the 2008 IEEE/PES Transmission and Distribution Conference and Exposition, Chicago, IL, USA, 21–24 April 2008.
5. Sannino, A.; Postiglione, G.; Bollen, M.H.J. Feasibility of a DC network for commercial facilities. *IEEE Trans. Ind. Appl.* **2003**, *39*, 1499–1507. [[CrossRef](#)]
6. Anand, S.; Fernandes, B.G. Optimal voltage level for DC microgrids. In Proceedings of the IECON 2010—36th Annual Conference on IEEE Industrial Electronics Society, Glendale, AZ, USA, 7–10 November 2010; pp. 3034–3039.
7. Fregosi, D.; Ravula, S.; Brhlik, D.; Saussele, J.; Frank, S.; Bonnema, E.; Scheib, J.; Wilson, E. A comparative study of DC and AC microgrids in commercial buildings across different climates and operating profiles. In Proceedings of the 2015 IEEE First International Conference on DC Microgrids (ICDCM), Atlanta, GA, USA, 7–10 June 2015; pp. 159–164.
8. Backhaus, S.; Swift, G.W.; Chatzivasileiadis, S.; Tschudi, W.; Glover, S.; Starke, M.; Wang, J.; Yue, M.; Hammerstrom, D. *DC Microgrids Scoping Study: Estimate of Technical and Economic Benefits*; Los Alamos National Lab.: Los Alamos, NM, USA, 2015; pp. 1–94.
9. Li, H.; Li, S.; Wang, T.; Wang, X.; Chang, X.; Zhang, M.; Meng, R. A Comparison of Energy Efficiency in AC and DC Microgrid with New Energy. *IOP Conf. Ser. Earth Environ. Sci.* **2020**, *619*, 012057.
10. Dastgeer, F.; Gelani, H.E. A Comparative analysis of system efficiency for AC and DC residential power distribution paradigms. *Energy Build.* **2017**, *138*, 648–654. [[CrossRef](#)]
11. Gerber, D.L.; Vossos, V.; Feng, W.; Marnay, C.; Nordman, B.; Brown, R. A simulation-based efficiency comparison of AC and DC power distribution networks in commercial buildings. *Appl. Energy* **2018**, *210*, 1167–1187. [[CrossRef](#)]
12. Gelani, H.E.; Dastgeer, F. Efficiency analyses of a DC residential power distribution system for the modern home. *Adv. Electr. Comput. Eng.* **2015**, *15*, 135–142. [[CrossRef](#)]
13. Gelani, H.E.; Dastgeer, F.; Siraj, K.; Nasir, M.; Niazi, K.A.K.; Yang, Y. Efficiency comparison of AC and DC distribution networks for modern residential localities. *Appl. Sci.* **2019**, *9*, 582. [[CrossRef](#)]
14. Ahmad, F.; Dastgeer, F.; Gelani, H.E.; Khan, S.; Nasir, M. Comparative analyses of residential building efficiency for AC and DC distribution networks. *Bull. Pol. Acad. Sci. Tech. Sci.* **2021**, *69*, 2021.
15. Anees, H.M.; Kazmi, S.A.A.; Naqvi, M.; Naqvi, S.R.; Dastgeer, F.; Gelani, H.E. A mathematical model-based approach for DC multi-microgrid performance evaluations considering intermittent distributed energy resources, energy storage, multiple load classes, and system components variations. *Energy Sci. Eng.* **2021**, *9*, 1919–1934. [[CrossRef](#)]
16. Gelani, H.E.; Dastgeer, F.; Shah, S.A.A.; Saeed, F.; Yousuf, M.H.; Afzal, H.M.W.; Bilal, A.; Chowdhury, M.S.; Techato, K.; Channumsin, S.; et al. Comparative Efficiency and Sensitivity Analysis of AC and DC Power Distribution Paradigms for Residential Localities. *Sustainability* **2022**, *14*, 8220. [[CrossRef](#)]
17. Mughees, M.; Sadaf, M.; Gelani, H.E.; Bilal, A.; Saeed, F. Comparison of Efficiency Based Optimal Load Distribution for Modular Ssts With Biologically Inspired Optimization Algorithms. *Electronics* **2022**, *11*, 1988. [[CrossRef](#)]
18. Gelani, H.E.; Khan, S.; Dastgeer, F.; Idrees, Z.; Afzal, M.W.; Nasir, M. System efficiency for AC vs. DC distribution paradigms: A comparative evaluation. *Bull. Pol. Acad. Sci. Tech. Sci.* **2022**, *70*, 139956. [[CrossRef](#)]
19. Gelani, H.E.; Dastgeer, F.; Nasir, M.; Khan, S.; Guerrero, J.M. AC vs. DC Distribution Efficiency: Are We on the Right Path? *Energies* **2021**, *14*, 4039. [[CrossRef](#)]
20. Dastgeer, F.; Anees, H.M.; Gelani, H.E.; Amjad, K.; Arif, R. A basic mathematical testbed for energy efficiency analyses of DC power distribution systems/microgrids. *Bull. Electr. Eng. Inform.* **2021**, *10*, 1484–1494. [[CrossRef](#)]

21. Tahir, H.; Gelani, H.E.; Idrees, Z.; Kim, R.Y. Techno-economic analysis of energy storage devices for microgrid's ramp rate control using bi-level evaluation method. *J. Energy Storage* **2022**, *55*, 105745. [[CrossRef](#)]
22. Saputra, F.W.Y.; Aripriharta; Fadlika, I.; Mufti, N.; Wibowo, K.H.; Jong, G.J. Efficiency Comparison between DC and AC Grid Toward Green Energy in Indonesia. In Proceedings of the 2019 IEEE International Conference on Automatic Control and Intelligent Systems (I2CACIS), Selangor, Malaysia, 29 June 2019; pp. 129–134.
23. Thomas, B.A.; Azevedo, L.; Morgan, G. Edison Revisited: Should we use DC circuits for lighting in commercial buildings? *Energy Policy* **2012**, *45*, 399–411. [[CrossRef](#)]
24. Glasgow, B.; Lima, I.; Hendrickson, C. How much electricity can we save by using direct current circuits in homes? Understanding the potential for electricity savings and assessing feasibility of a transition towards DC powered buildings. *Appl. Energy* **2016**, *180*, 66–75.
25. Tahir, H.; Lee, J.S.; Kim, R.Y. Efficiency evaluation of the microgrid for selection of common bus using copula function-based efficiency curves of the converters. *Sustain. Energy Technol. Assess.* **2021**, *48*, 101621. [[CrossRef](#)]
26. Renita Pinto, B.A.R. Reliability Analysis of Converters. *Int. J. Innov. Res. Electr. Electron. Instrum. Control Eng.* **2016**, *3*. [[CrossRef](#)]
27. Shi, X.; Bazzi, A.M. Reliability modeling and analysis of a micro-grid with significant clean energy penetration. In Proceedings of the 2015 9th International Conference on Power Electronics and ECCE Asia (ICPE-ECCE Asia), Seoul, Republic of Korea, 1–5 June 2015; pp. 202–207.
28. Baschel, S.; Koubli, E.; Roy, J.; Gottschalg, R. Impact of component reliability on large scale photovoltaic systems' Performance. *Energies* **2018**, *11*, 1579. [[CrossRef](#)]
29. Sayed, A.; El-Shimy, M.; El-Metwally, M.; Elshahed, M. Reliability, availability and maintainability analysis for grid-connected solar photovoltaic systems. *Energies* **2019**, *12*, 1213. [[CrossRef](#)]
30. Shrestha, B.R.; Tamrakar, U.; Hansen, T.M.; Bhattarai, B.P.; James, S.; Tonkoski, R. Efficiency and Reliability Analyses of AC and 380V DC Distribution in Data Centers. *IEEE Access* **2018**, *6*, 63305–63315. [[CrossRef](#)]
31. Ansari, O.A.; Safari, N.; Chung, C.Y. Reliability assessment of microgrid with renewable generation and prioritized loads. In Proceedings of the 2016 IEEE Green Energy and Systems Conference (IGSEC), Long Beach, CA, USA, 6–7 November 2016. [[CrossRef](#)]
32. Sandelic, M.; Peyghami, S.; Sangwongwanich, A.; Blaabjerg, F. Reliability aspects in microgrid design and planning: Status and power electronics-induced challenges. *Renew. Sustain. Energy Rev.* **2022**, *159*, 112127. [[CrossRef](#)]
33. Linhao, Y.; Ke, W.; Xu, C.; Tingcheng, H.; Mengying, L. Reliability Evaluation of Microgrid Considering Electric Vehicles and Demand Response. In Proceedings of the 2018 International Conference on Power System Technology (POWERCON), Guangzhou, China, 6–8 November 2018; pp. 1668–1672. [[CrossRef](#)]
34. Escalera, A.; Prodanovic, M.; Segovia, R.; Castronuovo, E.D. Reliability Evaluation of Grid-Connected Microgrids with High Penetration of Renewable Distributed Energy Resources. In Proceedings of the CIRED 2018 Ljubljana Workshop, Ljubljana, Slovenia, 7–8 June 2018.
35. Adefarati, T.; Bansal, R.C.; Justo, J.J. Reliability and economic evaluation of a microgrid power system. *Energy Procedia* **2017**, *142*, 43–48. [[CrossRef](#)]
36. Tahir, H.; Park, D.H.; Park, S.S.; Kim, R.Y. Optimal ESS size calculation for ramp rate control of grid-connected microgrid based on the selection of accurate representative days. *Int. J. Electr. Power Energy Syst.* **2022**, *139*, 108000. [[CrossRef](#)]
37. Ertugrul, N.; Abbott, D. DC is the Future [Point of View]. *Proc. IEEE* **2020**, *108*, 615–624. [[CrossRef](#)]
38. Duarte, G.; Rolim, C.; Baptista, P. How battery electric vehicles can contribute to sustainable urban logistics: A real-world application in Lisbon, Portugal. *Sustain. Energy Technol. Assess.* **2016**, *15*, 71–78. [[CrossRef](#)]
39. Bamisile, O.; Obiora, S.; Huang, Q.; Okonkwo, E.C.; Olagoke, O.; Shokanbi, A.; Kumar, R. Towards a sustainable and cleaner environment in China: Dynamic analysis of vehicle-to-grid, batteries and hydro storage for optimal RE integration. *Sustain. Energy Technol. Assess.* **2020**, *42*, 100872. [[CrossRef](#)]
40. Yang, X.; Zhang, Y.; Zhang, F.; Xu, C.; Yi, B. Enhancing Utilization of PV Energy in Building Microgrids via Autonomous Demand Response. *IEEE Access* **2021**, *9*, 23554–23564. [[CrossRef](#)]
41. Mehdi Hakimi, S.; Hajizadeh, A.; Shafie-khah, M.; Catalão, J.P.S. Demand Response and Flexible Management to Improve Microgrids Energy Efficiency with a High Share of Renewable Resources. *Sustain. Energy Technol. Assess.* **2020**, *42*, 100848. [[CrossRef](#)]
42. Nikolaidis, P.; Poullikkas, A. Cost metrics of electrical energy storage technologies in potential power system operations. *Sustain. Energy Technol. Assess.* **2018**, *25*, 43–59. [[CrossRef](#)]
43. Chamandoust, H.; Bahramara, S.; Derakhshan, G. Day-ahead scheduling problem of smart micro-grid with high penetration of wind energy and demand side management strategies. *Sustain. Energy Technol. Assess.* **2020**, *40*, 100747. [[CrossRef](#)]
44. Marchgraber, J.; Gawlik, W.; Wailzer, G. Reducing SoC-Management and losses of battery energy storage systems during provision of frequency containment reserve. *J. Energy Storage* **2020**, *27*, 101107. [[CrossRef](#)]
45. Qian, H.; Lai, J.S.; Zhang, J.; Yu, W. High-efficiency bidirectional AC-DC converter for energy storage systems. In Proceedings of the 2010 IEEE Energy Conversion Congress and Exposition, Atlanta, GA, USA, 12–16 September 2010; pp. 3224–3229.
46. Islam, M.; Nasrin, M.; Sarkar, A.B. An isolated bidirectional DC-DC converter for energy storage systems. In Proceedings of the International Exhibition and Conference for Power Electronics, Intelligent Motion, Renewable Energy and Energy Management, Nuremberg, Germany, 16–18 May 2017; pp. 2–7.

47. Chen, Y.T.; Tsai, M.H.; Liang, R.H. DC-DC converter with high voltage gain and reduced switch stress. *IET Power Electron.* **2014**, *7*, 2564–2571. [[CrossRef](#)]
48. Fan, H.; Li, H. High-frequency transformer isolated bidirectional DC-DC converter modules with high efficiency over wide load range for 20 kVA solid-state transformer. *IEEE Trans. Power Electron.* **2011**, *26*, 3599–3608. [[CrossRef](#)]
49. Scarabelot, L.T.; Rambo, C.R.; Rampinelli, G.A. A relative power-based adaptive hybrid model for DC/AC average inverter efficiency of photovoltaics systems. *Renew. Sustain. Energy Rev.* **2018**, *92*, 470–477. [[CrossRef](#)]
50. Kim, H.S.; Ryu, M.H.; Baek, J.W.; Jung, J.H. High-efficiency isolated bidirectional AC-DC converter for a DC distribution system. *IEEE Trans. Power Electron.* **2013**, *28*, 1642–1654. [[CrossRef](#)]
51. *IEEE Standard 493-2207; Design of Reliable Industrial and Commercial Power Systems.* IEEE: New York, NY, USA, 2007.
52. Defence, D. *Reliability Prediction of Electronic Equipment (Military Handbook)*; U.S. Department of Defense: Washington, DC, USA, 1991.
53. Electromaps Charging Stations in South Korea. Available online: <https://www.electromaps.com/en/charging-stations/south-korea> (accessed on 14 September 2020).
54. Xing, Q.; Chen, Z.; Zhang, Z.; Huang, X.; Leng, Z.; Sun, K.; Chen, Y.; Wang, H. Charging demand forecasting model for electric vehicles based on online ride-hailing trip data. *IEEE Access* **2019**, *7*, 137390–137409. [[CrossRef](#)]
55. Doosan Fuel Cell Technology. Available online: <https://www.doosanfuelcell.com/en/prod/prod-0101/> (accessed on 14 September 2020).
56. Prabhala, V.A.K.; Baddipadiga, B.P.; Ferdowsi, M. DC distribution systems—An overview. In Proceedings of the 2014 International Conference on Renewable Energy Research and Application (ICRERA), Milwaukee, WI, USA, 19–22 October 2014; pp. 307–312.
57. Rodriguez-Diaz, E.; Chen, F.; Vasquez, J.C.; Guerrero, J.M.; Burgos, R.; Boroyevich, D. Voltage-Level Selection of Future Two-Level LVdc Distribution Grids: A Compromise between Grid Compatibility, Safety, and Efficiency. *IEEE Electr. Mag.* **2016**, *4*, 20–28. [[CrossRef](#)]
58. Afamefuna, D.; Chung, I.Y.; Hur, D.; Kim, J.Y.; Cho, J. A techno-economic feasibility analysis on LVDC distribution system for rural electrification in South Korea. *J. Electr. Eng. Technol.* **2014**, *9*, 1501–1510. [[CrossRef](#)]
59. ILJIN Electric. *Overhead Transmission Line*; ILJIN Electric: Seoul, Republic of Korea, 2015; ISBN 8241413300.
60. Zhang, H. Key Technologies and Development Challenges of High-proportion Renewable Energy Power Systems. *Highlights Sci. Eng. Technol.* **2023**, *29*, 137–142. [[CrossRef](#)]

Disclaimer/Publisher’s Note: The statements, opinions and data contained in all publications are solely those of the individual author(s) and contributor(s) and not of MDPI and/or the editor(s). MDPI and/or the editor(s) disclaim responsibility for any injury to people or property resulting from any ideas, methods, instructions or products referred to in the content.